scientific reports

Check for updates

OPEN

Mesoporous silica nanoparticles co-loaded with lysozyme and vancomycin for synergistic antimicrobial action

Nasrin Namdar[1], Bahar Nayeri Fasaei[2]✉, Parvin Shariati[1], Seyed Mehdi Joghataei[2]✉ & Ayyoob Arpanaei[1,3]✉

Nanotechnology offers a novel strategy for enhancing the susceptibility of pathogens resistant to traditional antibiotics. Another effective strategy is combination therapy, where multiple agents are used together to improve treatment efficacy. In this study, both nanoparticle-based formulation and combinatorial therapy were utilized to develop a potent antibacterial system targeting infectious bacteria. Lysozyme (Lys) and Vancomycin (Van) were co-loaded onto mesoporous silica nanoparticles (MSNs), forming Lys-Van-MSNs. The antimicrobial activity of these nanoparticles was evaluated by determining the minimum inhibitory concentration (MIC) against *Staphylococcus aureus*. The MIC values for Lys-Van-MSNs were 0.85 µg/ml for Van and 0.168 mg/ml for Lys, reflecting reductions of 86.4% and 93.7%, respectively, compared to the free forms. Additionally, cytotoxicity was tested using MTT, ROS, and hemolysis assays on human cell lines (breast, fibroblast, and AGS), showing over 80% cell viability, indicating minimal toxicity. The MSN-based formulation, with its synergistic antibacterial effects, reduced drug dosage, and high biocompatibility, offers a practical and effective solution for addressing bacterial infections.

Keywords Nanoparticles, MSNs, Combination therapy, Lysozyme, Vancomycin

Antibiotic resistance has caused significant global health issues. According to a statistical report, antibiotic resistance could lead to an annual mortality rate of 700,000 people[1,2]. The discovery of new antibiotic classes has stalled since 1984, creating an urgent need for better strategies to address the potential threat of large-scale bacterial resistance outbreaks[3,4]. High-priority pathogens that require immediate attention include Methicillin-resistant *Staphylococcus aureus* (MRSA)[5], *Clostridium difficile*, *Carbapenem-resistant Enterobacteriaceae* (CRE), and multidrug-resistant *Acinetobacter*[5,6]. Bacterial resistance mechanisms typically involve several processes: bacteria may produce enzymes like hydrolases to inactivate antibiotics before they reach their target sites, alter their outer membrane permeability to prevent antibiotic entry or overexpress efflux pumps to expel antibiotics from the cell. Furthermore, they can modify target proteins to reduce antibiotic binding[7,8]. Designing new drug delivery systems, such as nanocarriers, can overcome the first three resistance mechanisms by effectively protecting antibiotics from enzymatic degradation[3,9,10].

Most bacteria can specifically recognize antibiotics or limit their access to the cell interior through degradation or exocytosis, indicating the development of drug resistance over time or in response to high doses[10,11]. However, new drug delivery systems, such as nanomaterials, can protect the active compounds, allowing significant amounts of antibiotics to enter bacterial cells undetected[12]. These nanostructures have sparked considerable interest among pharmaceutical researchers in using nano-delivery systems to enhance the antibacterial efficacy of antibiotics[13,14]. These systems help revive existing antibiotics by preventing hydrolysis, improving uptake, and bypassing efflux pumps, thereby overcoming resistance barriers[2,15]. Among these systems, Mesoporous Silica Nanoparticles (MSNs) have garnered significant attention due to their high drug-loading capacity, large surface area and pore volume, easy surface modification, stability, tunable properties, and biocompatibility. MSNs can significantly improve antibiotic delivery to bacteria by controlling shape, modifying surface properties, and reducing particle size[3,16,17].

[1]Department of Industrial and Environmental Biotechnology, National Institute of Genetic Engineering and Biotechnology (NIGEB), Tehran, Iran. [2]Department of Microbiology and Immunology, Faculty of Veterinary Medicine, University of Tehran, Tehran, Iran. [3]Scion, Private Bag 3020, Rotorua 3046, New Zealand. ✉email: nayerib@ut.ac.ir; mehdi.joghataei@ut.ac.ir; ayyoob.arpanaei@scionresearch.com

Thanks to the exceptional properties of MSNs, their versatile applications show great potential in tackling the global challenge of antimicrobial resistance[18,19]. Combination therapy, which involves using multiple therapeutic agents simultaneously, is another approach to enhance treatment efficacy[15,20,21]. Numerous studies have explored antimicrobial nano-delivery systems by loading Vancomycin (Van) or Lysozyme (Lys) individually onto nanoparticles to increase antimicrobial activity and reduce the required drug dose[22]. However, no prior research has examined the combined effect of co-loading Lys and Van onto MSNs. Therefore, this study was conducted with the aim of leveraging combination therapy and the beneficial properties of MSNs, particularly their suitable surface for the co-loading of two antimicrobial agents. The stability and efficiency of Van and Lys, alongside their controlled release, determine the optimal conditions for loading them onto MSNs, which helps to evaluate the nano-delivery system's impact on bacteria and the interaction of Van and Lys in both free and loaded forms.

Materials and methods

Materials

Tetraethyl orthosilicate (TEOS) 99% (silica precursor) (Foreign Trade Commodity Code: 29209070900), Hexadecyltrimethylammonium bromide (CTAB) (Foreign Trade Commodity Code: 29239000900), ammonium hydroxide (NH_4OH), absolute ethanol, and hydrochloric acid were sourced from Merck, Germany. Deionized water was prepared using the Q-check controller system (Milli-Q water) from OES Co., USA. Vancomycin hydrochloride and egg white lysozyme (629710G-F) were obtained from Sigma–Aldrich. Phosphate-buffered saline (PBS), *Staphylococcus aureus* (ATCC 6538P), and Brain Heart Infusion Broth were also from Merck, Germany. N-(2-aminoethyl)-3-aminopropyltrimethoxy-silane (AAPTMS), human fibroblast (Hf), human breast cancer (Hb), and human gastric cancer (AGS) cell lines were sourced from the National Institute of Genetic Engineering and Biotechnology, Iran. Fetal Bovine Serum (FBS) 10% was obtained from Invitrogen Co., USA, and DMEM 1X culture medium from Stem Cell Technology, Iran. Penicillin and streptomycin (1000 units/ml) and Trypan blue were from Sigma–Aldrich Co., USA. Trypsin 0.25% was supplied by BIO-IDEA Co., Iran, and Methyl Green, Sodium dodecyl sulfate (SDS), and N, N-dimethylformamide (DMF) were also from Sigma–Aldrich Co., USA.

Synthesis of mesoporous silica nanoparticles (MSNs)

MSNs were synthesized using the CTAB elimination method (Stober's method) as outlined in Gounani's study (Fig. 1)[23]. In brief, 300 µl of 2 N NH_4OH was added to an aqueous solution of CTAB (0.1 g, 48.65 ml Milli-Q water, final pH 11.5), and the mixture was heated to 80 °C while stirring at 1500 rpm. TEOS was then gradually added, and the solution was stirred for two hours to form bare MSNs (B-MSNs). The mixture was then centrifuged (19000 × g for 20 min), and the isolated nanoparticles were introduced into a CTAB elimination solution (a mixture of HCl and absolute ethanol (0.99%) in a 1:10 ratio), followed by stirring at 70 °C overnight. The resulting B-MSNs were washed three times with absolute ethanol (99.99%)[1].

Characterization of MSNs

The average size, size distribution, and morphology of MSNs were analyzed using scanning transmission electron microscopy (STEM) with a HITACHI S5500 electron microscope operating at 30 kV. ImageJ software was used to assess the average size and size distribution from SEM images, measuring 300 nanoparticles per sample. Additionally, a Zetasizer Nano instrument equipped with a dynamic light scattering (DLS) system (Malvern Instruments, S90, UK) was employed to determine the MSNs' hydrodynamic diameters and zeta (ζ) potential.

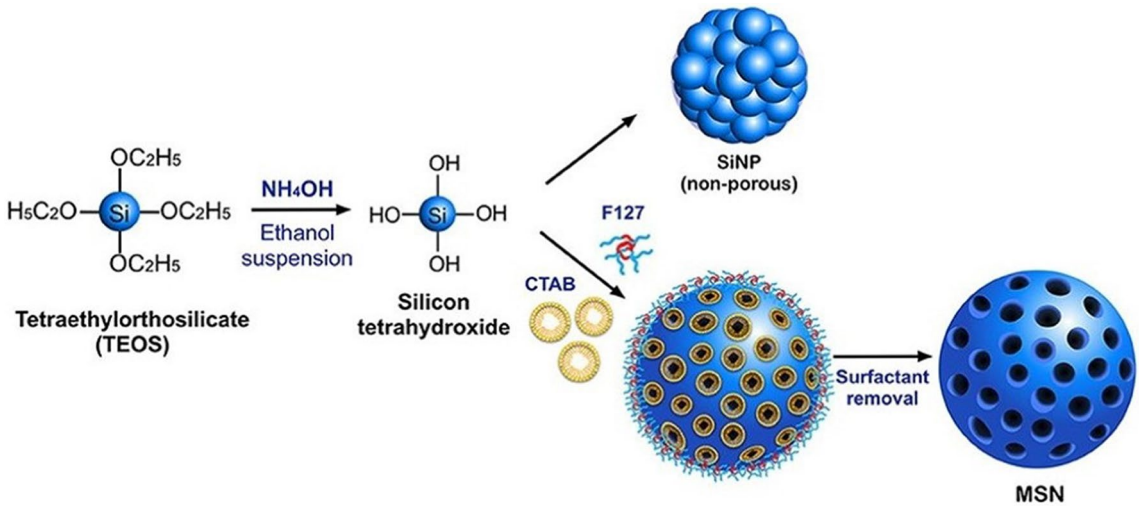

Fig. 1. Schematic representation of the synthesis of MSNs (Stober's method)[24].

The effect of buffer on the lys and Van loading onto MSNs

Two buffers were used to evaluate the effect of buffer on Lys and Van adsorption: a PBS stock solution (150 mM) and a tenfold diluted PBS solution (15 mM, pH 7.4). MSNs (1 mg) were sonicated twice for at least 30 min in 1 ml of the selected buffer (10 mM). The MSNs were then centrifuged and resuspended in 1 ml of each buffer containing 0.1 mg of Van and 1 mg of Lys. The suspensions were incubated on a rotary shaker (30 rpm) at 4 °C overnight. After incubation, the suspensions were centrifuged and washed with fresh buffer to remove loosely bound drug molecules, allowing determination of the final drug loading efficiency. The supernatants were collected and analyzed to measure the remaining Lys and Van by determining the drug concentration using a Varioskan Flash Multimode Reader (Thermo Scientific, Waltham, MA) at a wavelength of 220 nm. The amount of Lys and Van loaded onto MSNs was calculated by subtracting the remaining concentration from the initial concentration.

Adsorption of Lys and Van on MSNs

To assess the loading capacity and efficiency of Lys and Van onto MSNs, nanoparticle suspensions (1 mg/mL) were prepared in PBS buffer (1/10, 15 mM, pH 7.5) and sonicated for at least 30 min. Following this, various concentrations of Van (0.05, 0.1, 0.2, 0.4, 0.6 µg/mL) and Lys (0.25, 0.5, 1, 2, 3 mg/mL) were separately added to the MSN suspension (Fig. 2). The suspensions were incubated overnight on a rotary shaker (30 rpm) at room temperature. The next day, the suspensions were centrifuged (13000 × g for 20 min), resuspended in 1 ml PBS buffer, and centrifuged again to remove any loosely adsorbed Lys and Van. The supernatants were collected, and all experiments were performed in triplicate. The resulting nanoparticles were combined with 1 mL of PBS and stored at 4 °C. UV-Vis spectrophotometry, using a Varioskan Flash Multimode Reader at 220 nm, was employed to determine the concentrations of Lys and Van, allowing the calculation of non-adsorbed molecules. Loading efficiency (LE) and loading capacity (LC) of Lys and Van were calculated using Eqs. (1) and (2), respectively.

$$\text{LoadingEfficiency}\,(\%) = \left[\frac{\text{the total mass of applied Lys or Van} - \text{mass of no absorbed Lys or Van}}{\text{massofnoabsorbedLysorVan}}\right] \times 100 \quad (1)$$

$$\text{LoadingCapacity}\,(\mu\text{g/mg}) = \left[\frac{\text{the total mass of applied Lys or Van} - \text{themass of no absorbed Lys or Van}}{\text{totalmassofappliedMSNs}}\right] \times 100 \quad (2)$$

Lys and Van released from MSNs

The release profile was evaluated for MSNs loaded in PBS buffer (1/10, 15 mM, pH 7.5). Based on the findings from the previous section, 1 mg of samples preloaded with Lys and Van were suspended in 1 ml PBS and

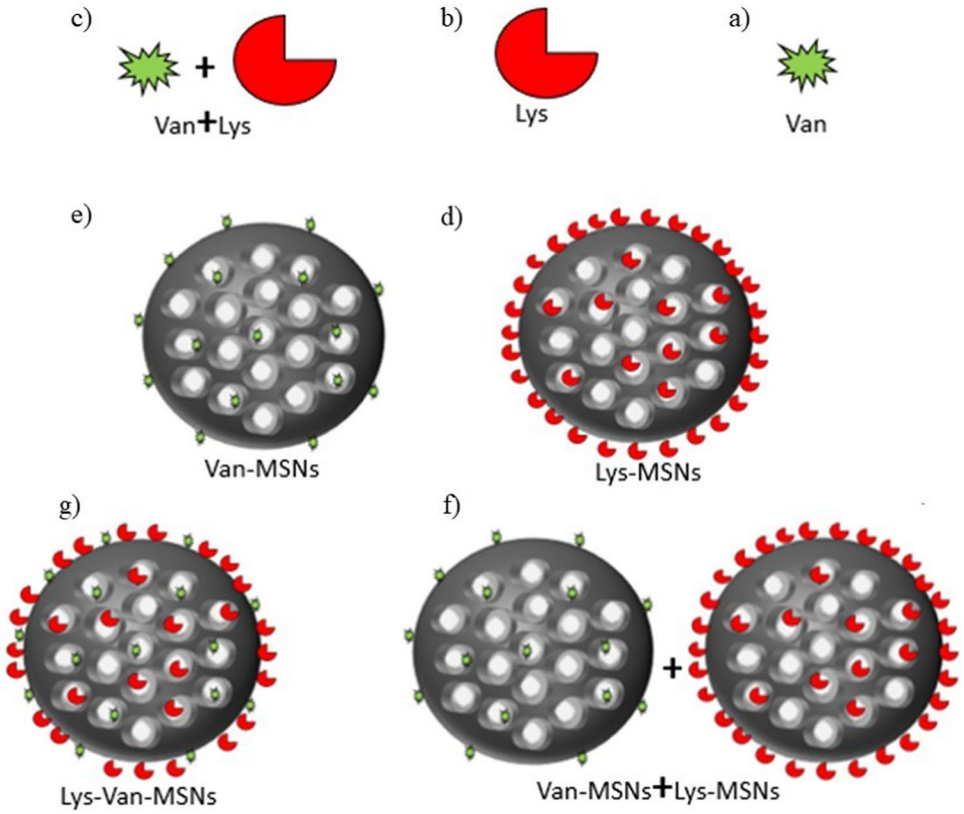

Fig. 2. Illustration of how various Van and Lys combinations are loaded onto MSNs. (**a**) Van; (**b**) Lys; (**c**) Van + Lys; (**d**) Lys–MSNs; (**e**) Van–MSNs; (**f**) Lys-MSNs + Van-MSNs; (**g**) Lys-Van-MSNs.

incubated at 200 rpm and 37 °C at various time intervals (0, 2, 4, 8, 12, 24, 48, 72 h). At each time point, samples were centrifuged at 19,000 × g for 20 min, and the drug content in the supernatants was measured using a Varioskan Flash Multimode Reader at 220 nm. The percentage of the released antibacterial agent was calculated by comparing the measured content to the initial loaded amount using a standard curve, and the release curve was plotted over time.

Co-loading of Lys and Van onto MSNs

Three co-loading methods were explored to determine the optimal Van and Lys co-loading configuration on the surface of MSNs. The ratios for Lys and Van were 1:1 (1 mg of MSNs:1 mg of Lys) and 1:0.1 (1 mg of MSNs: 100 µg of Van). The three co-loading approaches included: loading Lys first followed by Van (Lys–Van–MSNs), loading Van first followed by Lys (Van–Lys–MSNs) (Fig. 2), and simultaneous loading of both Lys and Van (Van–MSNs–Lys), all performed in PBS buffer (1/10, 15 mM, pH 7.5) at 4 °C.

Measuring the antibacterial properties of MSNs

In 4 mL of BHI medium, various concentrations of MSNs (0, 50, 100, 200, 400, 800, 1600, 3200 µg/mL) were individually exposed to 1.5×10^8 CFU of *S. aureus* (ATCC 6538P). The cultures were incubated in a shaker incubator at 37 °C and 180 rpm for 24 h. A culture without MSNs was used as a positive control. The optical density of the bacterial biomass was then measured at 600 nm using a Varioskan Flash Multimode Reader and compared to the control culture without MSNs.

Minimum inhibitory concentration (MIC) and Minimum Bactericidal Concentration (MBC) assays

The minimum inhibitory concentration (MIC) and minimum bactericidal concentration (MBC) were determined following the guidelines of the Clinical and Laboratory Standards Institute (CLSI) using the standard broth microdilution method[25]. The antimicrobial activity of Free Van at concentrations of 0, 0.195, 0.39, 0.781, 1.562, 3.125, 6.25, 12.5 µg/mL, Free Lys at 0, 0.168, 0.327, 0.675, 1.35, 2.7, 5.4, 10.8 mg/mL, a combination of Van and Lys at the same concentrations, Van–MSNs at 0, 0.195, 0.39, 0.781, 1.562, 3.125, 6.25, 12.5 µg/mL, Lys–MSNs at 0, 0.168, 0.327, 0.675, 1.35, 2.7, 5.4, 10.8 mg/mL, combined Lys–MSNs and Van–MSNs, and various concentrations of Van-Lys-MSNs (Van to Lys ratio 1 µg/mL:200 mg/mL; 0.85/0.168, 0.68/0.1344, 0.55/0.107, 0.4/0.086, 0.34/0.68, 0.27/0.0544, 0.02/0.047, 0) were tested against *S. aureus* (ATCC 6538P). A single colony of *S. aureus* was inoculated into MHB and incubated overnight at 37 °C and 180 rpm for 18 h. Serial dilutions were prepared in MHB in 96-well plates, inoculated with 1×10^6 CFU/mL bacteria from the overnight culture, and incubated at 37 °C for 24 h. Sterility controls (pure medium) and positive growth controls (broth without antibiotics but inoculated with bacteria) were also included. Bacterial growth was monitored by OD600 readings using a Varioskan Flash Multimode Reader. The MIC was defined as the lowest concentration with no visible turbidity. The MBC was determined by transferring 10 µl from wells with no visible growth onto fresh BHI plates, incubating at 37 °C for three days, and observing any viable cell growth. The MBC was the concentration at which no growth was observed, indicating a > 1000-fold reduction in CFU.

Fractional inhibitory concentration (FIC) and FIC Index (FICI) assays

The synergy between Lys and Van was evaluated using the checkerboard broth microdilution method[26]. The FIC was calculated based on the MIC values obtained from the previous section, using Eq. (3), and the FICI was determined using Eq. (4). The FICI results were interpreted following the European Committee for Antimicrobial Susceptibility Testing (EUCAST) guidelines. The interpretation was as follows: FICI ≤ 0.5 indicates synergy, 0.5 < FICI ≤ 1 indicates an additive effect, 1 < FICI ≤ 2 suggests indifference, and FICI > 2 indicates antagonism.

$$\mathrm{FIC} = \frac{\mathrm{MIC\ (A)\ in\ combination\ with\ MSNs}}{\mathrm{MIC\ (A)\ alone}} \tag{3}$$

$$\mathrm{FICI} = \mathrm{FIC\ (A)} + \mathrm{FIC\ (B)} \tag{4}$$

Evaluating the stability of loaded Lys and Van during preservation time

In order to assess the stability of the drug over the preservation period, concentrations equivalent to the MIC values of free and MSN-loaded Van and Lys were prepared in BHI culture medium inoculated with *S. aureus* (ATCC 6538P). These samples were stored at 25 °C and 4 °C for 0, 2, 4, 8, 12, 24, 48, and 72 h. Absorbance was measured in each group using UV – vis spectrophotometry (Varioskan Flash Multimode Reader) at 625 nm. The percentage of bacterial inhibition was then calculated using Eq. (5)[27].

$$\text{Bacterial inhibition}\ (\%) = \left[\frac{\text{The OD value of the control} - \text{OD value of the sample}}{\text{The OD value of the control}}\right] \times 100 \tag{5}$$

Cytotoxicity assays

MTT assay

Human fibroblast cell line (Hf), Human breast cancer cell line (Hb), and Human gastric cancer cell line (AGS) were plated in 96 well culture plates at a density of 1×10^4 cells/mL in 200 µl DMEM (Dulbecco's modified Eagle's medium) growth medium Contains 10% FBS, 100 units/ml of penicillin and 100 mg/ml of streptomycin and incubated overnight at 37 °C in 5% CO2 with 90% humidity. The top culture medium of each well was replaced after 24 h, when the cells had filled about 80% of it, with a fresh culture media containing the opposing substances. These fresh mediums included different concentrations of MSNs (0, 50, 100, 200, 400, 800, 1600, 3200 µg/mL),

MIC values of Van and Lys in combination, and free, loaded, and co-loaded states. For each concentration, three wells were designated. And incubation was carried out. In the following, the viability of the cells was evaluated using the MTT reduction method. The cells were incubated with 100 µl of 3-(4, 5-dimethylthiazol-2-yl)-2, 5-diphenyltetrazolium bromide (MTT) solution for four hours. The medium was removed, and the dark blue crystal was dissolved by adding 100 µl dimethyl sulfoxide. Also, free MSNs were separately assayed under the same condition at rates of 10, 25, 50, 100, 250, 500, 1000, and 1500 µg/mL (50,100,200,400,800,1600,3200 µg ml-1). Varioskan Flash Multimode Reader used an optical density of 570 nm to monitor cell viability. The Relative cell viability was calculated according to Eq. (6).

$$\text{Cell viability } (\%) = \left[\frac{\text{OD treated}}{\text{OD control}}\right] \times 100 \tag{6}$$

ROS assay

After treatment of Hf, Hb, and HAGS cells with different concentrations of MSNs (0, 50, 100, 200, 400, 800, 1600, 3200 µg/mL), MIC concentrations of Van and Lys in combination and free, loaded, and co-loaded state for 48 h, the cells were washed twice with PBS and then loaded with DCFH-DA 40 µM diluted in serum-free medium and incubated at 37 °C for two hours. The fluorescence intensities were detected using a Varioskan Flash Multimode Reader, with an excitation wavelength of 490 nm and an emission wavelength of 527 nm. Fluorescent intensities normalized with positive control of 100 µM H2O2 were incubated with DCFH-DA[28]. The ROS generation of cells was calculated according to Eq. (6).

Hemolytic assay

A total of 100 µL of MSNs up to 1500 µg/ml, MIC value of Van and Lys in combination and free, loaded, and co-loaded state are spread on the surface of a blood agar plate and incubated for 24 h at 37 ∘C. An equivalent of 1×106 CFU/ml of S. aureus was used as a control. The absence of detectable hemolysis was considered a sign of biocompatibility.

The effect of prepared antibacterial agents on the morphology of *S. aureus*

S. aureus was imaged using SEM under three different conditions: treated with Van and Lys at their MIC values, treated with Van-Lys-MSNs, and under untreated conditions.

Results and discussion

Characteristics of the manufactured MSNs

The synthesis and characterization of MSNs reveal critical insights into their size, structure, and potential applications. The average size of MSNs, as determined by SEM, was 77.22 ± 8.2 nm (Fig. 3A), while DLS indicated a larger average diameter of approximately 92 ± 10 nm. The MSNs were spherical with a regular size distribution (Fig. 3B). This discrepancy is attributed to the hydrodynamic nature of DLS measurements, which typically yield larger sizes than actual particle dimensions[29]. These results confirm that the "CTAB elimination method" effectively produces porous MSNs within the expected size range, with size regulation achievable through parameters such as ammonium hydroxide concentration, mixing speed, and TEOS addition rate[24,30]. Various structure-directing agents, such as CTAB and MTAB, influence the size and surface area[17,31]. In previous studies, the mean pore diameter and specific surface area were found to be 4.1 nm and 882.1 m^2/g, respectively[23,32]. While the findings underscore the effectiveness of the CTAB method in producing MSNs within the desired size range, it is essential to consider the implications of size discrepancies in practical applications, particularly in drug delivery systems where precise sizing can influence therapeutic efficacy.

Due to the abundance of oxygen and hydroxyl groups on the surface of silicon nanoparticles, they have a negative surface charge. ζ potential measurements of particles in deionized water evaluated the surface functionalization of MSNs. The surface charge of MSNs was approximately − 28.8 mV (Fig. 4A). Van and Lys are two positively charged molecules that can be surface absorbable at neutral pH thanks to the surface charge of MSNs. The high biocompatibility and chemical stability of MSNs as Nanocarriers, as well as their high loading capacity (thanks to the distinctive pore lattice) and simple functionalization (because of the presence of silanol groups – a functional group in silicon chemistry with the connectivity Si–O–H), are their main advantages. Additionally, using a variety of techniques, these nanoparticles can be easily synthesized in large quantities while exhibiting varying morphologies, pore sizes, surface functionalities, and lattices, thus demonstrating the incredible versatility of these Nano-systems[33–35].

Numerous protocols can be used to create silica nanoparticles (SiNPs), ranging in size from 10 to 500 nm, and come in various shapes and physicochemical properties. The Stober's process and the micro-emulsion method are the two most popular techniques for synthesizing SiNPs. The synthesis of monodispersed silica particles in the sub-micrometer range, the Stober method, was first used in 1968. This technique utilizes a TEOS, a silica precursor, which undergoes hydrolysis in the presence of ethanol and NH2OH, followed by a polycondensation reaction to produce non-porous silica particles with sizes less than 200 nm. A modified Stober's process incorporating surfactants like CTAB is frequently used to create MSN with pores. For various therapeutic and biomedical applications, these porous compartments are commonly used to load multiple drugs and biological molecules[24,36].

In line with recent advancements, Hongxing et al. (2024) demonstrated an efficient thiol-ene click reaction method to synthesize magnetic mesoporous silica ion-imprinted polymers (IIPs). The modified Stober's process used in our study aligns with the environmentally friendly approach outlined by Hongxing et al., demonstrating the adaptability of mesoporous silica nanoparticles (MSNs) for diverse applications. While our synthesis focused on drug delivery, the success of Hongxing et al. in selectively capturing Pb(II) ions from wastewaters highlights

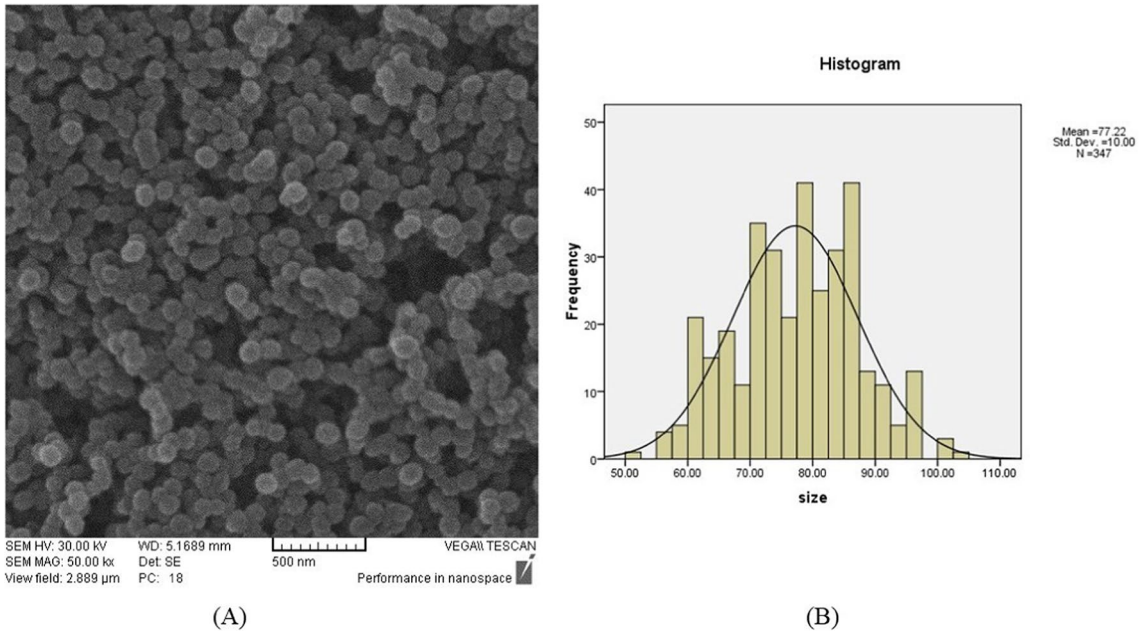

Fig. 3. SEM images of MSNs (**A**) along with their size distribution curve in nanometers (**B**).

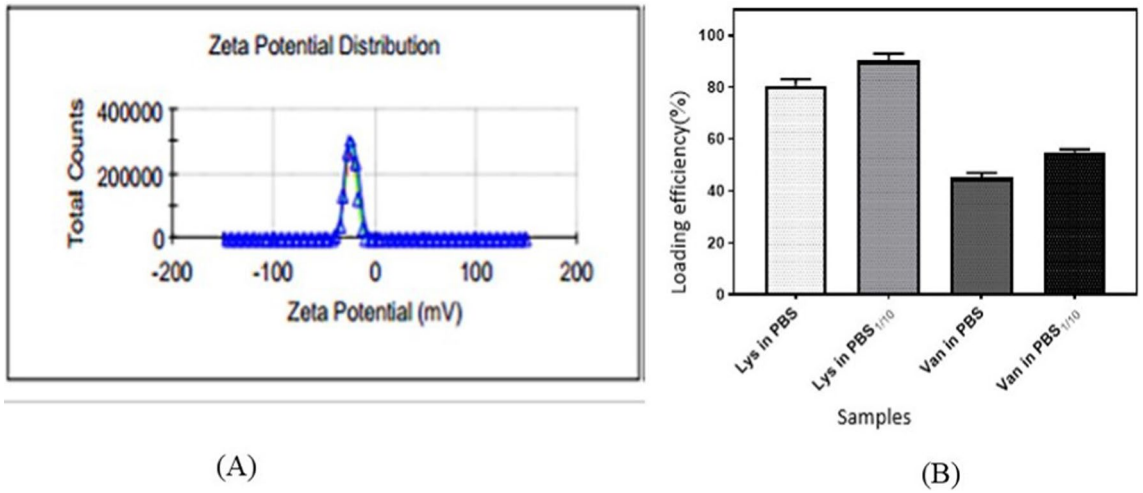

Fig. 4. Variation of the ζ–potential of MSNs (**A**). The effect of buffer on the Lys and Van loading onto MSNs (**B**).

the versatility of MSNs in other critical areas, such as environmental remediation. The thiol-ene click reaction method they employed could be further explored in future studies to enhance the functionalization of MSNs in biomedical contexts, ensuring rapid and efficient delivery systems with minimal side effects. Similarly, the precise control over pore structure, combined with the imprinted polymer approach, may offer insights into improving the selectivity and loading capacity of therapeutic agents in our applications. The innovative methods presented, particularly in regulating the binding sites for selective capture, provide an exciting avenue for further research into functionalizing MSNs for targeted delivery systems[37].

The results of Adsorption of Lys and Van on MSNs

The effect of buffer on the lys and Van loading onto MSNs

Investigations were conducted into how lowering the PBS buffer concentration affected the ability of van and lys to load onto MSNs. Van and Lys are physically absorbed by nanoparticles primarily due to their electrostatic attraction; by dilution, the ionic strength of the buffer can be decreased, increasing the electrostatic forces. Thus, it is possible to increase the above two compounds' absorption on MSNs in this way. According to the findings, the loading efficiency of Van and Lys on MSNs in PBS buffer (1/10) (15 mM) at pH 7.4 is about 10% more than that in undiluted PBS (150 mM) (Fig. 4B). The charged groups in the adsorbed molecule and on the

adsorbent's surface are covered by ions with various charges at higher concentrations in buffers, which reduces the electrostatic forces and surface absorption[38].

The effect of Lys and Van initial concentration on drug loading capacity and efficiency of MSNs
The effect of Van's initial concentration on adsorption was assessed at a range of 0.05–0.6 µg/mL, and Lys in 0.25-3 mg/mL at pH 7.5. In the relative mass values of 0.1:1 Van (1 mg of MSNs: 100 µg of Van) and the ratio of 1:1 Lys (1 mg of MSNs:1 mg of Lys), The highest LE and LC for Van 53.6% and 53.6 µg/mg, respectively, as well as for Lys 88.33% and 88.3 µg/mg, were obtained. The obtained results also demonstrate that while LE did not significantly decrease when Lys concentration was increased to 1 mg/ mL, it significantly reduced as concentration rose. This finding is most likely the result of high concentrations of Lys saturating nanoparticles and forming a complete protein halo[39]. The LE and LC of various Lys and Van concentrations on MSNs are depicted in Fig. 5A.

Results of Lys and Van's release from MSNs

The Van release rate from the nanoparticle surface is very high in the first 8 h (about 77%), and it then continues slowly until 72 h, as the release isotherm demonstrates (Fig. 4B). The weak electrostatic forces of adsorption between MSNs and Van molecules in the PBS buffer may be the primary cause of this observation, as previously explained[40] and additionally observed that in the case of Lys, the rate of release from MSNs' surfaces is meager during the first 8 h and rises to about 20% after 72 h (Fig. 5B). Due to its high isoelectric point and the more vital electrostatic attraction forces created between positively charged Lys molecules and negatively charged MSNs surface at pH 7.4, the release of lys may also be slower than Van's. The strength and amount of electrostatic attraction forces are generally mentioned in the sources as affecting drug loading and release[40,41].

Results of measuring the Antibacterial properties of MSNs

The findings demonstrated that MSNs do not significantly inhibit the growth of *S. aureus* up to a concentration of 100 µg/ml, and up until this concentration, the growth rate is roughly 80% of what it would be without nanoparticles. However, the inhibitory effect significantly increased as MSN concentration rose. So, the cell mass was reduced to about 50% at 3200 µg/ml (Fig. 6).

Antibacterial activity results

S. aureus exhibited slower growth as the concentration of both combined and free Van and Lys increased. However, the MIC values were lower when Van and Lys were combined, meaning bacterial growth was inhibited at a much lower concentration. The MIC values for free Van and Lys were 6.25 µg/ml and 2.7 mg/ml, respectively. In the combined Van + Lys state, the MIC values dropped to 1.56 µg/ml for Van and 0.675 mg/ml for Lys (Fig. 7A). For Van-MSNs, the MIC was 3.125 µg/ml, and for Lys-MSNs, it was 0.675 mg/ml. In the Lys-MSNs + Van-MSNs state, the MIC values were 0.781 µg/ml for Van and 0.168 mg/ml for Lys (Fig. 77). For the Van-Lys-MSNs formulation, the MIC values were 0.85 µg/ml for Vav and 0.168 mg/ml for Lys. The MIC and MBC values are summarized in Table 1.

The analysis revealed statistically significant reductions in MIC values ($p < 0.05$) when Van and Lys were combined or loaded onto MSNs, highlighting the enhanced antibacterial efficacy of these formulations. For Van, the MIC decreased by 75% when combined with Lys (Van + Lys) compared to free Van, by 50% when loaded

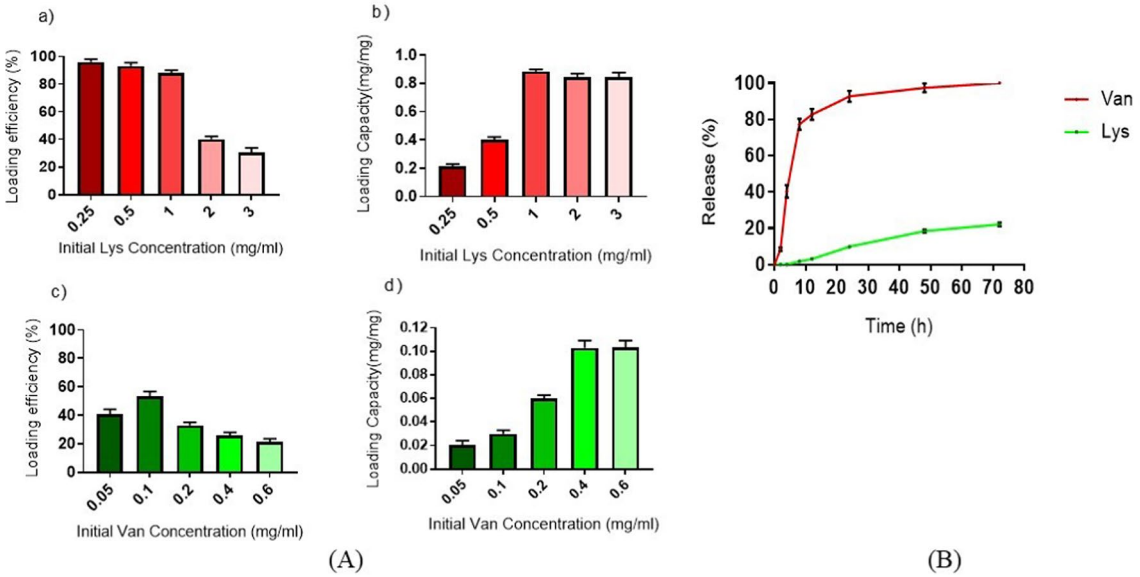

Fig. 5. (**A**): (**a**), Loading efficiency of Lys; (**b**), Loading Capacity of Lys; (**c**), Loading efficiency of Van; (**d**), Loading Capacity of Van. (**B**): The Van and Lys releasing curve as a function of time in PBS buffer (pH 7.4) duration 72 h.

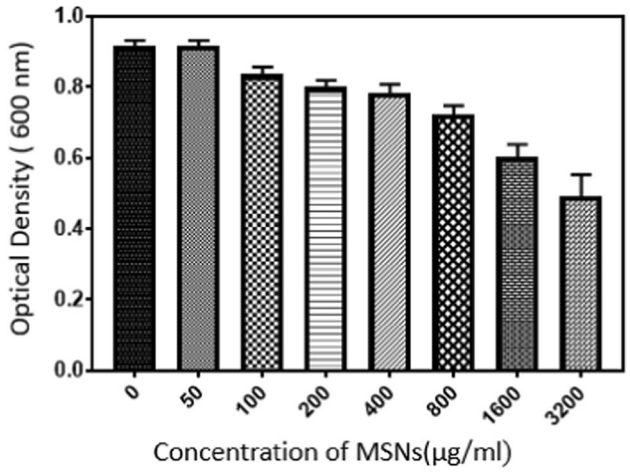

Fig. 6. Antibacterial effects (Optical density) of MSNs in different concentrations on the growth and proliferation of *S. aureus* during 24 h.

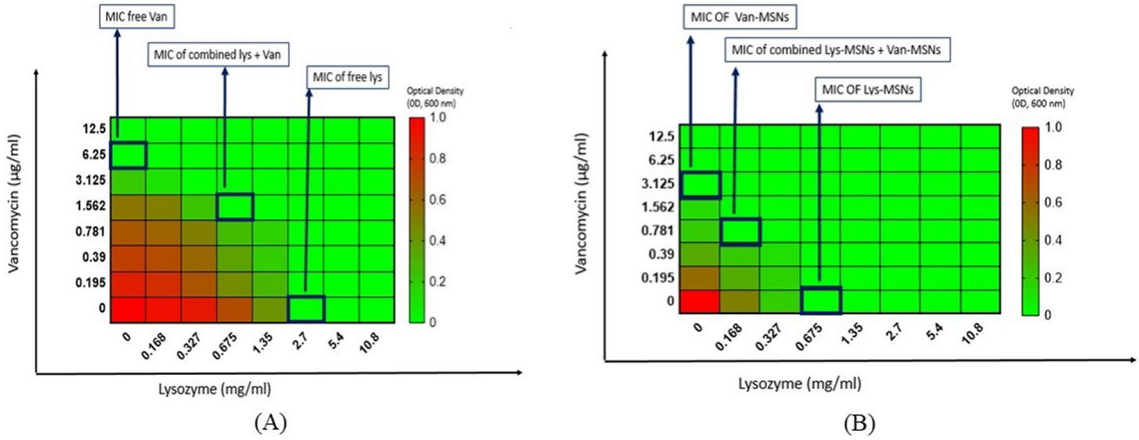

Fig. 7. MIC of free Van, free Lys, and Van + Lys (**A**); Van-MSNs, Lys-MSNs, and Lys-MSNs + Van-MSNs (**B**).

Row	Compound	MIC ($Van_{(\mu g/ml)}/Lys_{(mg/ml)}$)	MBC ($Van_{(\mu g/ml)}/Lys_{(mg/ml)}$)
1	Lys	– / 2.7	– / 10.8
2	Van	6.25 / –	25 / –
3	Lys + Van	1.562 / 0.675	1.562 / 0.675
4	Lys-MSNs	– / 0.675	– / 10.8
5	Van-MSNs	3.125 / –	12.5 / –
6	Lys-MSNs + Van-MSNs	0.781 / 0.168	5.4 / 3.125
7	Van-Lys-MSNs	0.85 / 0.168	1.35 / 6.837

Table 1. MIC and MBC values for different compounds.

onto MSNs (Van-MSNs), by 87.5% in the Lys-MSNs + Van-MSNs formulation, and by 86.4% in the Van-Lys-MSNs formulation. Similarly, the MIC for Lys dropped by 75% in the combined Van + Lys state compared to free Lys when loaded onto MSNs (Lys-MSNs) and by 93.8% in both the Lys-MSNs + Van-MSNs and Van-Lys-MSNs formulations. These results demonstrate the substantial increase in antibacterial efficacy when both Van and Lys are combined or loaded onto MSNs, leading to significant reductions in the concentrations required to inhibit bacterial growth.

The MBC value for free Van was found to be 25 µg/ml. However, even when the concentration of free Lys was increased up to 10.8 mg/ml, bacterial growth, though minimal, was still observed (Fig. 8A). This finding indicates that the MBC value for Lys could not be determined within the concentration range tested. Previous

studies have similarly noted that Lys is not bactericidal[42]. In the combined Van + Lys treatment, the MBC values for Van and Lys were 6.25 µg/ml and 10.8 mg/ml, respectively (Fig. 6A). For Van-MSNs, the MBC was 12.5 µg/ml, but the MBC for Lys-MSNs could not be calculated, as bacterial growth was still present even at 10.8 mg/ml. In the Lys-MSNs + Van-MSNs formulation, no bacterial growth was observed at concentrations of 3.125 µg/ml for Van and 5.4 mg/ml for Lys (Fig. 8B).

There are two main reasons why antibacterial compounds are more effective when loaded onto nanoparticles rather than in their free form. First, loading Van and Lys onto MSNs stabilizes them in the environment. Second, it leads to the accumulation of Van and Lys at specific points on the bacterial cell surface, resulting in more effective destruction[43]. Nanoparticles facilitate the accumulation of antibacterial agents at specific sites on bacterial cells, enhancing their destructive capabilities. For instance, the functionalization of $ZnFe_2O_4$ nanoparticles with Van significantly improved its antibacterial activity against MRSA[44].

Additionally, the use of nanocarriers like niosomes and nanotubes has been shown to improve penetration into biofilms, allowing for higher local concentrations of antibiotics at infection sites[45,46]. SEM imaging of treated versus untreated cells offers evidence supporting the outlined mechanisms and explanations. The results indicate that, for antibacterial purposes, loading Van onto MSNs is more crucial than loading Lys, as free Van molecules are less stable than Lys. Loading Van onto nanoparticles enhances its stability, thereby improving its performance. Furthermore, the study demonstrated that the best antibacterial efficacy is achieved when both agents are combined in their loaded state on nanoparticles (Lys-MSNs + Van-MSNs), resulting in an 8-fold and 16-fold reduction in MIC values for Van and Lys, respectively, compared to their free state.

The best co-loading efficiency was when Van and Lys were first loaded into MSNs (Van-Lys-MSNs). Due to the very high adsorption rate of Lys on MSNs compared to Van, first, Van was adsorbed on MSNs, and then, MSNs carrying Van were placed in a solution containing Lys to absorb this compound as well. The absorption amount of Lys then Van was measured in MSNs, and the results showed that the absorption amount of Lys then Van is equal to their absorption amount in Lys-MSNs and Van-MSNs states. Co-loading was done to compare the antibacterial performance of two types of formulations, one Lys-MSNs + Van-MSNs and the other Van-Lys-MSNs. In the state where the ratio of Van to Lys was 0.85 µg/ml and 0.168 mg/mL, respectively, bacterial growth was inhibited entirely (MIC) (Fig. 9A). In lower concentrations, bacterial growth was observed. Observations show that based on MIC, the antibacterial activity of Van-Lys-MSNs is not significantly different compared to Lys-MSNs + Van-MSNs. Respectively, Concentrations of 6.837 µg/ml and 1.35 mg/ml for Van and Lys were determined as MBC in Van-Lys-MSNs state (Fig. 9B).

In line with the findings of Nasaj et al., the current study highlights the potential of functionalized nanocomposites for enhancing antimicrobial efficacy. Nasaj et al. demonstrated that Fe3O4@SiO2@Chitosan nanocomposites functionalized with Van and nisin (a member of the class of cationic peptide antimicrobials) exhibited significant antibacterial effects against MRSA, both in vitro and in vivo. Their study showed that a polymer/drug ratio of 1:1 resulted in the slowest release rate of Van, improving sustained antimicrobial activity. Similarly, the present study focuses on the use of mesoporous silica nanoparticles (MSNs) as carriers for Van and Lys, which also exhibit controlled release profiles and synergistic antibacterial effects. Both studies reinforce the role of nanoparticle-based delivery systems in enhancing the therapeutic effectiveness of conventional antibiotics, suggesting their potential to overcome drug resistance and improve clinical outcomes[47]. Aligned with the findings of Rahaman et al., the present investigation similarly underscores the potential of nanoparticle-based drug delivery systems to fight against antibiotic-resistant *S. aureus*. Rahaman et al. demonstrated that the combination of Van and gallic acid loaded into mesoporous silica nanoparticles (MSNs) and amino-functionalized MSNs (AP-MSNs) showed enhanced antibacterial effects, with the AP-MSNs displaying better cell viability and biocompatibility. The synergistic action of Van and gallic acid significantly increased bacterial membrane damage and cell death, providing a promising strategy to address multidrug resistance. Similarly, our research focuses on using MSNs as a carrier for Van and Lys, achieving controlled release and synergistic antimicrobial effects. Both studies underscore the potential of combination therapy using nanocarriers to enhance the efficacy of conventional antibiotics and provide alternative therapeutic approaches to address drug-resistant bacterial infections [48].

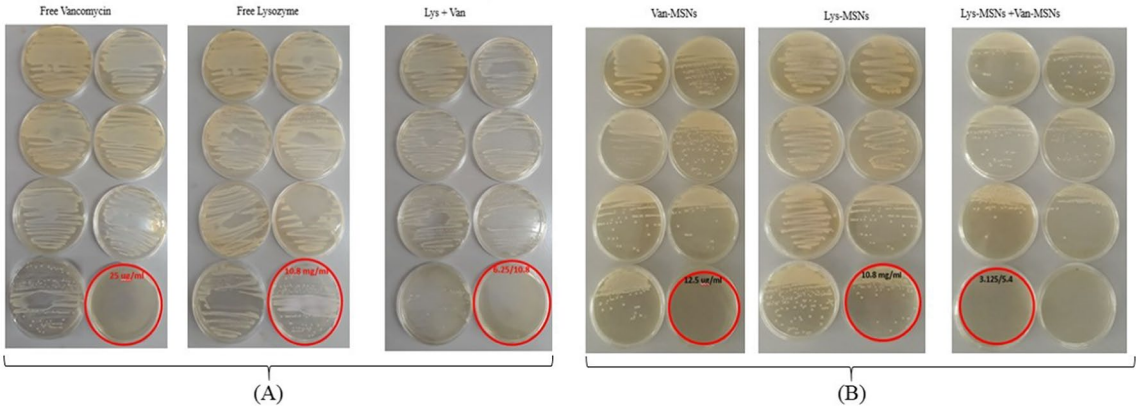

Fig. 8. MBC of free Van, free Lys, and Van + Lys (**A**); Van-MSNs, Lys-MSNs, and Lys-MSNs + Van-MSNs (**B**).

Row	Compound	FIC $_{(Van/Lys)}$	FICI	Interaction type
1	Van and Lys	0.25 / 0.25	0.5	Synergy
2	Van-MSNs and Lys-MSNs	0.25 / 0.25	0.5	Synergy

Table 2. The results of FIC and FICI indicators.

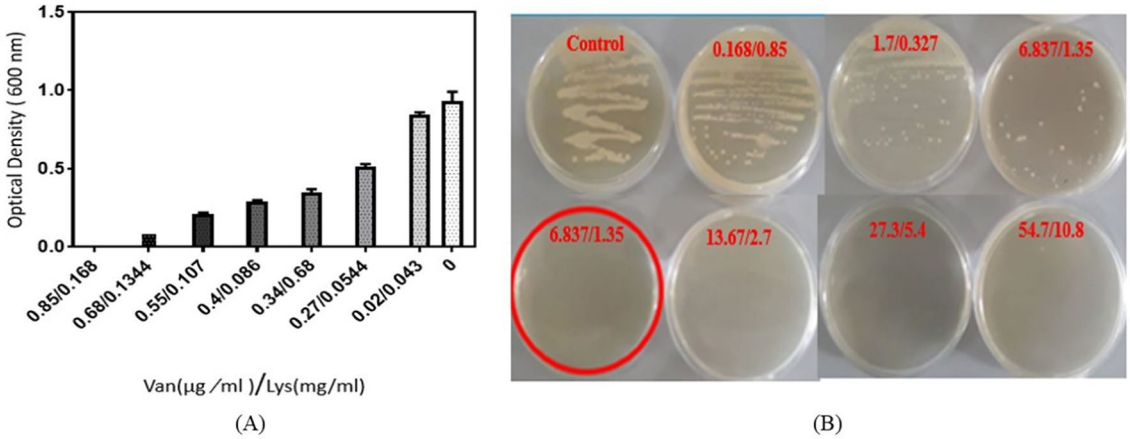

Fig. 9. MIC for Van–Lys–MSNs (**A**); MIC plates for Van–Lys–MSNs (**B**). (Van (μg/ml)/Lys (mg/ml)).

FIC and FICI results

Based on calculations, the FICI value between Van and Lys was equal to 0.5. Also, the FICI value between Van-MSNs and Lys-MSNs was equivalent to 0.5 (Table 2). These values demonstrate the synergistic relationship between the antibacterial agents.

The results of examining the morphology of *S. aureus* by SEM

The images of *S. aureus* cells (Fig. 10A) treated with Van and Lys in their free state at their MIC concentrations (1.562 μg/ml and 0.675 mg/ml, respectively) showed that some cells' cell walls and membranes were severely damaged. A pale fluid-like mass can be seen near the damaged areas of these cells, which is most likely caused by cytoplasmic content leakage. Also, the bacterial cells' abnormal structure and shape and their lengthening suggest that the division process has halted and prevented their growth and reproduction (Fig. 10B). These observations indicate that the presence of Van and Lys targets the cell wall and the membrane and thus has a synergistic effect. Following the treatment of bacterial cells with Van-Lys-MSNs, it is easy to see that the carrier MSNs are entirely attached to the surface of the bacterial cells, and a sizable accumulation surrounds the cells (Fig. 10C). This accumulation implies that Van and Lys, combined with this formulation with a much higher concentration, can accumulate on the surface of *S. aureus* and manifest their effects. The concentration of MSNs on the surface has increased, which leads to the accumulation of Van and Lys on the surface of the bacterial wall. Some MSNs have penetrated the bacterial cell, as seen in some parts of the SEM image. Nearly every cell was visible in the image; its cell wall was severely destroyed, and the cells were cluster-like, single, and elongated (Fig. 10C). Cell elongation indicates inhibition of cell division and growth.

The Lys's activity damages the polysaccharide chain of the peptidoglycan layer, which increases the likelihood that Van will enter the wall and then effectively bind it to D-alanine and D-alanine structure, leading to extensive cell destruction and significant synergy between the antibacterial compounds used. Van's further binding to D-alanine and D-alanine structure prevents the synthesis of cell walls. The cell wall is not strong due to the low content of peptide molecules that form a peptide bridge and can be more strongly affected by Lys, which can hydrolyze and destroy the cell[49–53]. In a 2013 study by Qi et al., it was found that Van loaded on silica nanoparticles could inhibit bacterial cell proliferation more effectively than free Van[54]. Popat et al. 's research in 2011 found that Lys loaded on the surface of silica nanoparticles can destroy the bacterial cell membrane more effectively than free Lys[41]. However, in the present study, it was demonstrated that the presence of Van and Lys synergistically can destroy bacterial cells and prevent their proliferation. The interaction of Van, Lys, and Van-Lys-MSNs with the *S. aureus* bacteria's cell wall and membrane is schematically depicted in Fig. 11.

The innovation and significance of this study stem from its development of MSNs as an effective drug delivery system, combined with the use of two antibacterial agents, offering a novel strategy to combat antibiotic resistance. While earlier studies have investigated the use of MSNs for cancer treatment or have examined drug delivery systems incorporating an antimicrobial agent, this research concentrates explicitly on their application in antimicrobial therapies, with a particular emphasis on the delivery of Lys and Van antibiotics[37]. The study's results, showing enhanced antibacterial performance with Van-Lys-MSNs, highlight the synergistic effect between sustained drug release and antibiotic diffusion. The MSNs synthesized in this study demonstrated a significant reduction in required antibiotic dosages while maintaining or enhancing therapeutic effects,

marking a substantial advancement in the development of nano-antibiotics. This research represents a step forward in engineering nano-platforms for targeted antimicrobial therapies, contributing to the evolving field of nanomedicine for infection control.

Stability of loaded Lys and Van during preservation time

According to the findings, all compounds gradually lost their antibacterial properties throughout a 72-hour storage period at 25 °C. The remarkable thing is that the antibacterial properties of free Van, free Lys, and Lys + Van were quickly decreased compared to the loaded and co-loaded compounds. The mentioned compounds' antibacterial activity decreased by about 20% after 24 h, while loaded and co-loaded compounds fell to about 50% of the initial value. In every instance, the antibacterial activity decreased much more slowly at 4 °C than at 25 °C. After 72 h at 4° C, Lys + Van and free Lys' antibacterial activity reached 50% of the initial value, while free Van, loaded, and co-loaded compounds reached only 100–80% of the initial value. Free Van's stability at 4° C was significantly superior to that of free Lys and Lys + Van. Van has a much smaller structure than Lys, contributing to Van's stability. That's why, unlike Lys, Van does not easily change its structure or reduce its activity when the temperature is low, such as 4 °C (Fig. 12). The findings of this section, along with results of

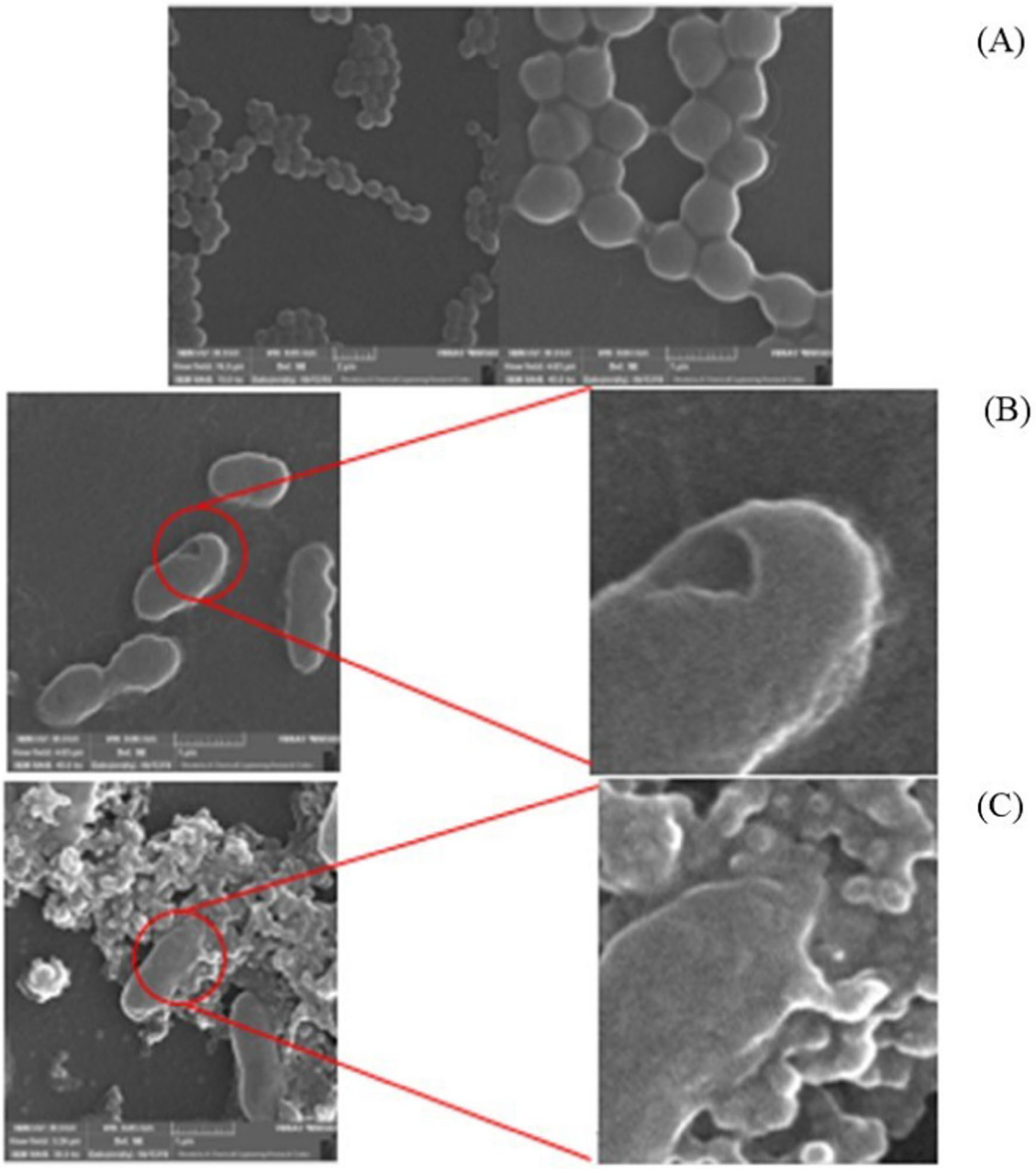

Fig. 10. SEM images of untreated *S. aureus* bacteria (**A**), treated with Van and Lys (**B**), treated with Van-Lys-MSNs (**C**).

MSN release and antibacterial activity, demonstrate that Van and Lys loaded on MSMs can gradually be released into the environment and significantly inhibit the growth of *S. aureus* bacteria while still maintaining their stability, particularly active structure of Lys due to surface adsorption.

Levofloxacin (LVX), gentamicin (GM), and rifampin (RIF) were each individually loaded into MSNs in the 2021 study by Aguilar-Colomer et al. For *S. aureus* and *E. coli*, the released antibiotic's biological activity curves were determined at different times. For LVX, RIF, and GM, sustained release above the MIC was seen to last up to 96 h. MSNs are excellent Nanocarriers for loading and releasing antibiotics from various families and maintaining their antimicrobial activity, as demonstrated by the study and current studies[55].

Cytotoxicity

The cytotoxicity of mammalian cells presents one of the main difficulties for antibacterial agents. The effects of agents on cell viability (MTT,) ROS formation, and RBC hemolysis were investigated to address these issues. MSNs up to a concentration of 800 µg/mL do not significantly affect cell lines toxically, according to the results of the MTT assay's examination of MSN cellular toxicity at various concentrations. Additionally, the cell lines' viability did not fall by more than 20% as the concentration rose to 3200 µg/mL (Fig. 13A). This observation is consistent with previous findings, which indicate MSNs are not intrinsically toxic[41,56–58]. Studies have also demonstrated that MSNs are less toxic in low doses than non-mesoporous silica nanoparticles[41]. No appreciable toxicity effects were seen with other prepared antibacterial agents, especially Van-Lys-MSNs (Fig. 13B). The fact that Lys and Van impact the peptidoglycan structure of bacterial cell walls may explain why these agents have no toxic effects on human cell lines. Human cells lack this structure, so antibacterial nano-systems have no harmful effects[59,60]. According to several earlier studies, anionic functionalized MSNs had less cell toxicity than cationic

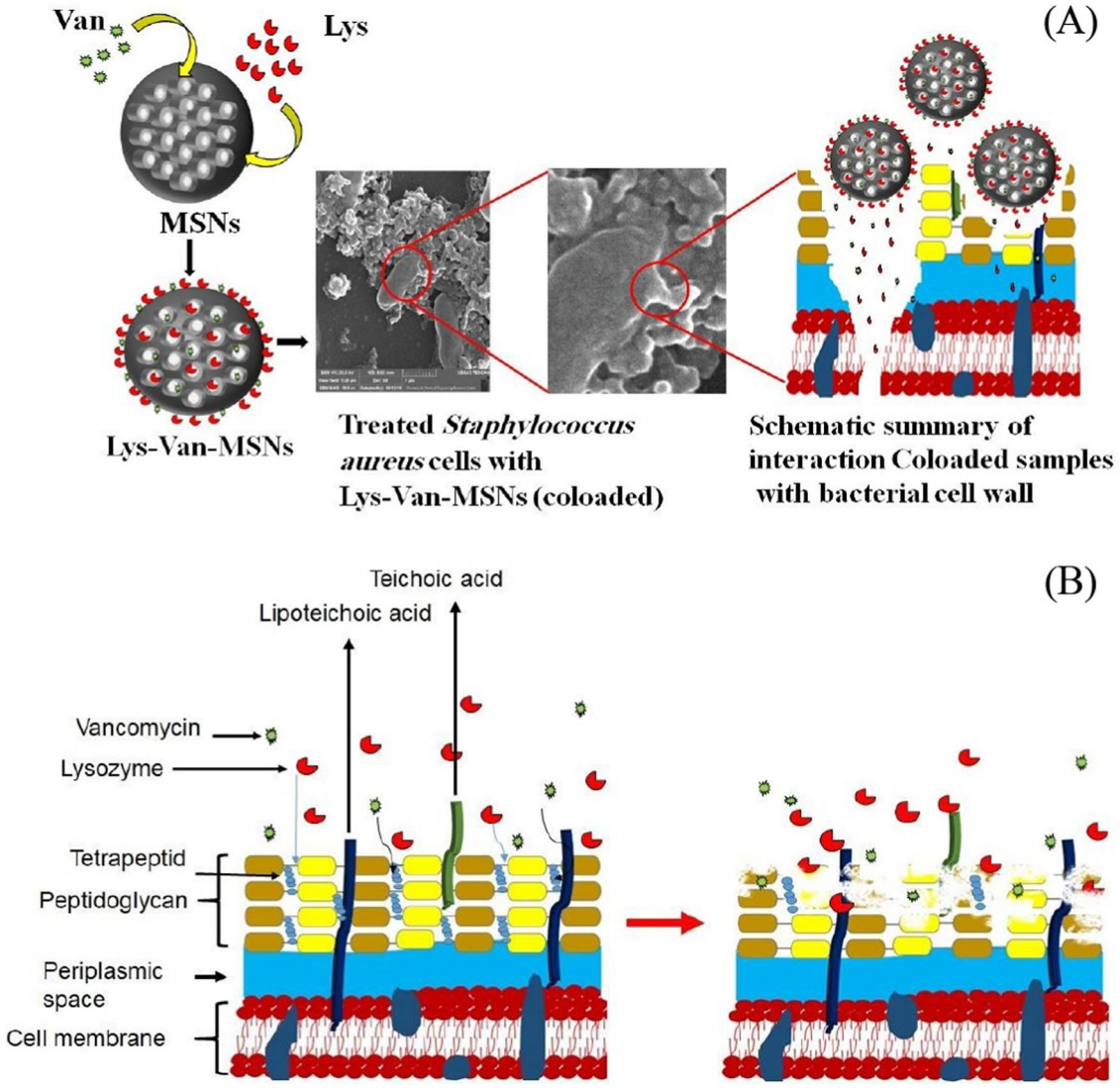

Fig. 11. Schematic interaction of Van-Lys MSNs (**A**) and free Van and free Lys (**B**) with the cell wall and membrane of *S. aureus* bacteria.

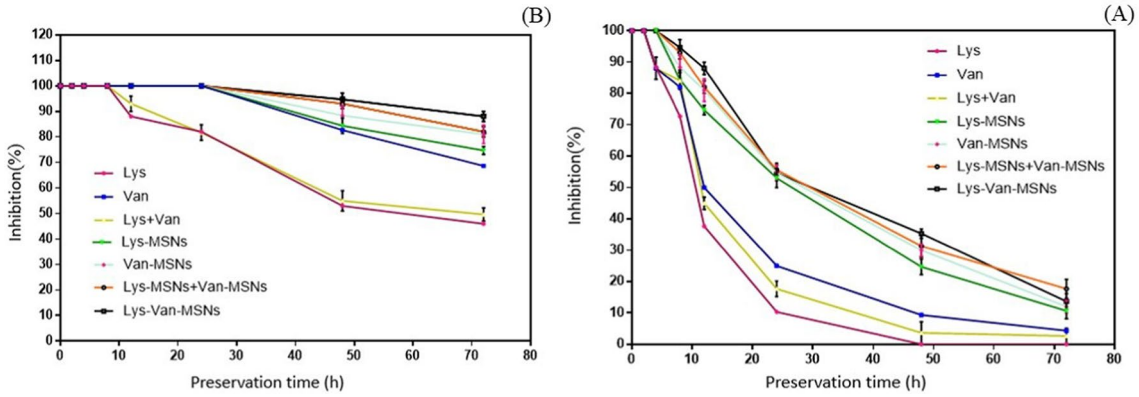

Fig. 12. Stability of investigated compounds during preservation time at 25 °C (**A**) and 4 °C (**B**).

functioned ones, which is a sign of these molecules' surface chemistry, charge dependence, and cell uptake and toxicities[56].

One of the main nanotoxicity mechanisms influenced by nanoparticle surface charges, surface chemistry, etc., is the formation of ROS[56,61]. The current study's findings demonstrated that MSNs in the concentrations under investigation do not significantly contribute to ROS formation (Fig. 13C). Studies indicate that MSNs, even at high concentrations (1.95–1000 µg/mL), do not significantly alter cell viability or ROS levels in rat pheochromocytoma PC12 cells[62]. Although amorphous, non-porous silica nanoparticles have been reported to have ROS induction properties, it is challenging to locate MSN reports that are comparable[63]. The examined cell lines do not significantly cause ROS formation when prepared antibacterial agents are present in various states (Free Van and free Lys state and loaded and co-loaded states) (Fig. 13D). There was no difference between free Van and free Lys state and loaded and co-loaded states, but in general, nanoparticles decrease the formation of ROS for some reasons, Firstly, nanoparticles may activate cell signaling pathways to increase expression of

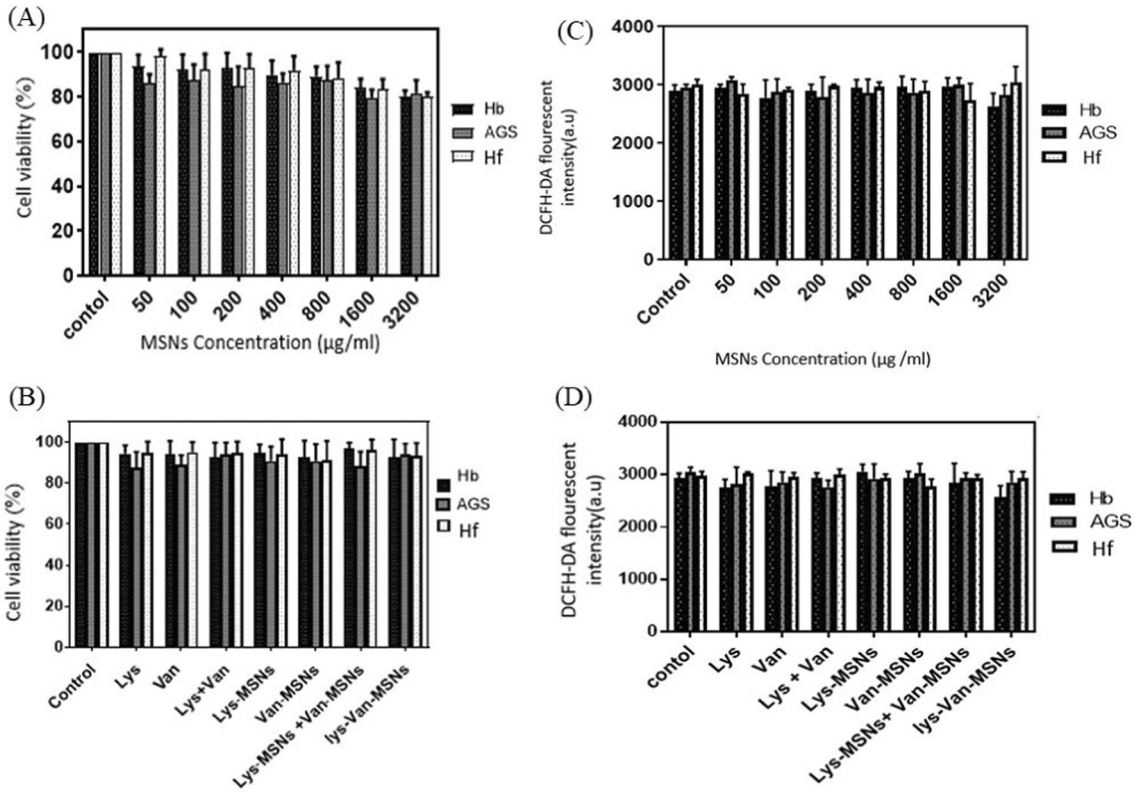

Fig. 13. Cell viability assay results for human fibroblast cells (Hf), human breast cancer cell line (Hb), Human gastric cancer cell line (AGS) using MTT and ROS assays. MTT assay results for MSNs at various concentrations (**A**) and MIC concentrations of prepared antibacterial agents (**B**); ROS assay results for MSNs at different concentrations (**C**) and MIC concentrations of prepared antibacterial agents (**D**).

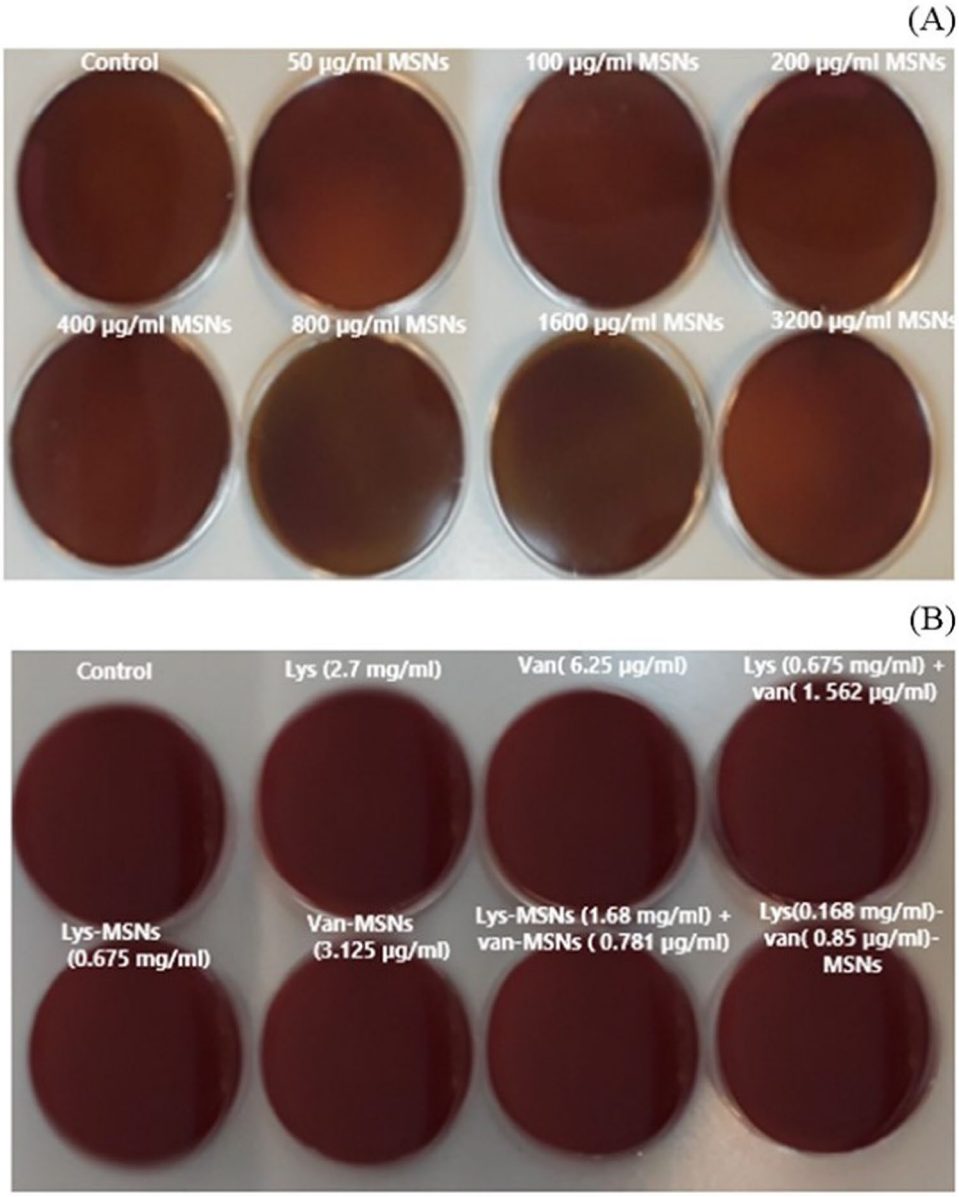

Fig. 14. Hemolytic assay results for MSNs in different concentrations (**A**) and MIC concentrations of prepared antibacterial agents (**B**).

endogenous antioxidant enzymes, and secondly, electron–electron polarization and forming a transfer complex with free radicals and reduction of mitochondrial ROS[64,65]. The hemolytic assay's findings concluded that MSNs in different concentrations (Fig. 14A) and MIC concentrations of prepared antibacterial agents (Fig. 14B) had no hemolytic effect.

Conclusion

In summary, the current study explored various strategies to enhance the antibacterial performance of MSNs, focusing on their unique properties and applications. The synthesized MSNs demonstrated favorable characteristics, such as uniform size distribution and good surface properties. Both Lys and Van were effectively loaded onto the MSNs, and the controlled diffusion and release of these antibiotics showed promising results. The Van-Lys-MSNs exhibited a more potent antimicrobial effect, which can be attributed to the synergistic action and sustained release of the loaded antibiotics, as observed in the study of their antibacterial activity against *S. aureus* and their morphological impact on the bacteria. The nanoparticles, produced in concentrations that inhibit bacterial growth, also displayed favorable cytotoxicity profiles. High doses or frequent administration of current antibiotics may increase their effectiveness but also lead to the rise of bacterial resistance and heightened toxicity. The synthesized MSNs in this study reduce the risk of antibiotic resistance and toxicity by lowering the necessary drug dosage. Additionally, their targeted delivery reduces the need for frequent doses, enhancing their

antimicrobial efficiency even at lower concentrations. The increased antibacterial activity of the nano-delivery system can be attributed to three key factors: (1) improving the therapeutic index to reduce dosing frequency, (2) enhancing intracellular drug delivery to slow down resistance, and (3) ensuring drug accumulation at targeted sites by altering pharmacokinetic behavior, thereby minimizing side effects[43,66,67].

This report emphasizes the role of MSNs as effective drug delivery systems with significant potential for treating infectious diseases. The current study contributes to the advancement of nano-antibiotics by leveraging comprehensive knowledge of mesoporous materials as drug carriers and utilizing advanced technologies to design nano-based solutions to combat infections. It highlights MSNs as versatile nano-platforms for developing targeted antimicrobial formulations for future bacterial infection therapies. Unlike cancer therapeutics, nanotechnology is still in its early stages for treating infectious diseases, and challenges such as bacterial and biofilm microenvironments, which differ by species, need to be addressed[2,24,35,43]. Investigating the antimicrobial properties of Van-Lys-MSNs on the growth of other gram-positive and gram-negative pathogenic bacteria, as well as evaluating their stability in acidic and alkaline conditions, will help advance drug delivery systems. Additionally, co-loading other antimicrobial compounds like methicillin and assessing the antibacterial performance and biocompatibility of Van-Lys-MSNs at various concentrations in vivo will further contribute to the development of effective treatment-responsive systems.

Data availability

The data generated and/or analyzed during the current study are available from the corresponding author on request.

Received: 30 June 2024; Accepted: 5 November 2024
Published online: 25 November 2024

References

1. Chaib, F., Butler, J. & Hwang, S. New report calls for urgent action to avert antimicrobial resistance crisis. *WHO NEWSLETTER, Joint News Release* (2019).
2. Wu, T. et al. Self-assembly multifunctional DNA tetrahedron for efficient elimination of antibiotic-resistant bacteria. *Aggregate* **5**, e402 (2024).
3. Zhuang, J., Yu, Y. & Lu, R. Mesoporous silica nanoparticles as carrier to overcome bacterial drug resistant barriers. *Int. J. Pharmaceut.*, 122529 (2022).
4. Hibbert, T. et al. Antimicrobials: An update on new strategies to diversify treatment for bacterial infections. *Adv. Microb. Physiol.* **84**, 135–241 (2024).
5. Xu, T. et al. Development of membrane-targeting fluorescent 2-Phenyl-1H-phenanthro[9,10-d]imidazole-antimicrobial peptide mimic conjugates against methicillin-resistant *Staphylococcus aureus*. *J. Med. Chem.* **67**, 9302–9317 (2024).
6. Organization, W. H. GLASS whole-genome sequencing for surveillance of antimicrobial resistance. (2020).
7. Uddin, T. M. et al. Antibiotic resistance in microbes: History, mechanisms, therapeutic strategies and future prospects. *J. Infect. Pub. Health* **14**, 1750–1766 (2021).
8. Darby, E. M. et al. Molecular mechanisms of antibiotic resistance revisited. *Nat. Rev. Microbiol.* **21**, 280–295 (2023).
9. Wang, Y. et al. Mesoporous silica nanoparticles in drug delivery and biomedical applications. *Nanomed. Nanotechnol. Biol. Med.* **11**, 313–327 (2015).
10. Chen, X. et al. Click-hydrogel delivered aggregation-induced emissive nanovesicles for simultaneous remodeling and antibiosis of deep burn wounds. *Aggregate* **5**, e406 (2024).
11. Stokes, J. M. et al. Pentamidine sensitizes gram-negative pathogens to antibiotics and overcomes acquired colistin resistance. *Nat. Microbiol.* **2**, 1–8 (2017).
12. Gupta, P. L., Rajput, M., Oza, T., Trivedi, U. & Sanghvi, G. Eminence of microbial products in cosmetic industry. *Nat. Prod. Bioprospect.* **9**, 267–278 (2019).
13. Wang, D.-Y., Van der Mei, H. C., Ren, Y., Busscher, H. J. & Shi, L. Lipid-based antimicrobial delivery-systems for the treatment of bacterial infections. *Front. Chem.* **7**, 872 (2020).
14. Vallet-Regi, M. & Tamanoi, F. Overview of studies regarding mesoporous silica nanomaterials and their biomedical application. *Enzymes* **43**, 1–10 (2018).
15. Izadi, A., Paknia, F., Roostaee, M., Mousavi, S. A. A. & Barani, M. Advancements in nanoparticle-based therapies for multidrug-resistant candidiasis infections: A comprehensive review. *Nanotechnology* **35**, 332001 (2024).
16. Narayan, R., Nayak, U. Y., Raichur, A. M. & Garg, S. Mesoporous silica nanoparticles: A comprehensive review on synthesis and recent advances. *Pharmaceutics* **10**, 118 (2018).
17. Feng, Y. et al. Mesoporous silica nanoparticles-based nanoplatforms: Basic construction, current state, and emerging applications in anticancer therapeutics. *Adv. Healthc. Mater.* **12**, 2201884 (2023).
18. Carvalho, G. C. et al. Highlights in mesoporous silica nanoparticles as a multifunctional controlled drug delivery nanoplatform for infectious diseases treatment. *Pharmaceut. Res.* **37**, 191 (2020).
19. Castillo, R. R. & Vallet-Regí, M. Recent advances toward the use of mesoporous silica nanoparticles for the treatment of bacterial infections. *Int. J. Nanomed.*, 4409–4430 (2021).
20. Si, Z., Pethe, K. & Chan-Park, M. B. Chemical basis of combination therapy to combat antibiotic resistance. *JACS Au* **3**, 276–292 (2023).
21. Majumder, S., Eckersall, P. D. & George, S. Bovine Mastitis: Examining factors contributing to treatment failure and prospects of nano-enabled antibacterial combination therapy. *ACS Agric. Sci. Technol.* (2023).
22. Li, B. et al. Powering mesoporous silica nanoparticles into bioactive nanoplatforms for antibacterial therapies: Strategies and challenges. *J. Nanobiotechnol.* **21**, 325 (2023).
23. Gounani, Z. et al. Mesoporous silica nanoparticles carrying multiple antibiotics provide enhanced synergistic effect and improved biocompatibility. *Colloids Surf. B Biointerfaces* **175**, 498–508 (2019).
24. Selvarajan, V., Obuobi, S. & Ee, P. L. R. Silica nanoparticles—a versatile tool for the treatment of bacterial infections. *Front. Chem.* **8**, 602 (2020).
25. Ugalde-Arbizu, M. *et al.* Antibacterial properties of mesoporous silica nanoparticles modified with fluoroquinolones and copper or silver species. *Pharmaceuticals* **16** (2023).
26. Alharthi, S., Ziora, Z. M., Janjua, T., Popat, A. & Moyle, P. M. Formulation and biological evaluation of mesoporous silica nanoparticles loaded with combinations of Sortase A inhibitors and antimicrobial peptides. *Pharmaceutics* **14** (2022).

27. Zhou, X. et al. Mesoporous silica nanoparticles/gelatin porous composite scaffolds with localized and sustained release of vancomycin for treatment of infected bone defects. *J. Mater. Chem. B* **6**, 740–752 (2018).
28. Zaidi, S., Misba, L. & Khan, A. U. Nano-therapeutics: A revolution in infection control in post antibiotic era. *Nanomed. Nanotechnol. Biol. Med.* **13**, 2281–2301 (2017).
29. Lorensia, A., Soedarsono, S., Suryadinata, R. V. & Badri, H. A. Effect of inhaler technique health education in improving symptoms and lung function in COPD outpatient in a private hospital in Gresik, Indonesia: Pilot studies. *Int. J. Drug Deliv. Technol. (IJDDT)* **14**, 768–776 (2024).
30. Kim, M. et al. Practical manipulation for the preparation of mesoporous silica nanoparticles for drug delivery vehicles. *Curr. Drug Deliv.* **20**, 1206–1215 (2023).
31. Hutem, A. & Yuenyao, C. in *Journal of Physics: Conference Series*. 012046 (IOP Publishing).
32. Behzadi, F. et al. Stability and antimicrobial activity of nisin-loaded mesoporous silica nanoparticles: A game-changer in the war against maleficent microbes. *J. Agric. Food Chem.* **66**, 4233–4243 (2018).
33. Zeng, M. et al. Scalable synthesis of multicomponent multifunctional inorganic core@ mesoporous silica shell nanocomposites. *Mater. Sci. Eng. C* **128**, 112272 (2021).
34. Castillo, R. R., de la Torre, L., García-Ochoa, F., Ladero, M. & Vallet-Regí, M. Production of MCM-41 nanoparticles with control of particle size and structural properties: Optimizing operational conditions during scale-up. *Int. J. Mol. Sci.* **21**, 7899 (2020).
35. Álvarez, E. et al. Nanoantibiotics based in mesoporous silica nanoparticles: New formulations for bacterial infection treatment. *Pharmaceutics* **13**, 2033 (2021).
36. Xu, J. et al. A facile cooling strategy for the preparation of silica nanoparticles with rough surface utilizing a modified Stöber system. *Coll. Surf. A Physicochem. Eng. Aspects* **625**, 126845 (2021).
37. He, H. et al. Synthesis of magnetic mesoporous silica adsorbents by thiol-ene click chemistry with optimised lewis base properties through molecular imprinting for the rapid and effective capture of Pb(II). *Chem. Eng. J.* **489**, 151294 (2024).
38. Konar, M., Mathew, A. & Dasgupta, S. Effect of silica nanoparticles on the amyloid fibrillation of lysozyme. *ACS Omega* **4**, 1015–1026 (2019).
39. Croissant, J. G., Fatieiev, Y., Almalik, A. & Khashab, N. M. Mesoporous silica and organosilica nanoparticles: Physical chemistry, biosafety, delivery strategies, and biomedical applications. *Adv. Healthc. Mater.* **7**, 1700831 (2018).
40. Kurczewska, J., Sawicka, P., Ratajczak, M., Gajęcka, M. & Schroeder, G. Vancomycin-modified silica: Synthesis, controlled release and biological activity of the drug. *Int. J. Pharmaceut.* **486**, 226–231 (2015).
41. Popat, A. et al. Mesoporous silica nanoparticles for bioadsorption, enzyme immobilisation, and delivery carriers. *Nanoscale* **3**, 2801–2818 (2011).
42. Wu, T. et al. Integration of lysozyme into chitosan nanoparticles for improving antibacterial activity. *Carbohyd. Polym.* **155**, 192–200 (2017).
43. Munir, M. U. & Ahmad, M. M. Nanomaterials aiming to tackle antibiotic-resistant bacteria. *Pharmaceutics* **14** (2022).
44. Akbari, M., Rezayan, A. H., Rastegar, H., Alebouyeh, M. & Yahyaei, M. Design and synthesis of vancomycin-functionalized $ZnFe_2O_4$ nanoparticles as an effective antibacterial agent against methicillin-resistant *Staphylococcus aureus*. *Drug Dev. Res.* **85**, e22148 (2024).
45. Hemmati, J. et al. Antibacterial and antibiofilm potentials of vancomycin-loaded niosomal drug delivery system against methicillin-resistant *Staphylococcus aureus* (MRSA) infections. *BMC Biotechnol.* **24**, 47 (2024).
46. Yan, H. et al. Enhancing biofilm penetration and antibiofilm efficacy with protein nanocarriers against pathogenic biofilms. *Int. J. Biol. Macromol.* **256**, 128300 (2024).
47. Nasaj, M. et al. Vancomycin and nisin-modified magnetic Fe_3O_4@SiO_2 nanostructures coated with chitosan to enhance antibacterial efficiency against methicillin resistant *Staphylococcus aureus* (MRSA) infection in a murine superficial wound model. *BMC Chem.* **18**, 43 (2024).
48. Rahaman, S. N., Ayyadurai, N. & Anandasadagopan, S. K. Synergistic effect of vancomycin and gallic acid loaded MCM-41 mesoporous silica nanoparticles for septic arthritis management. *J. Drug Deliv. Sci. Technol.* **82**, 104353 (2023).
49. Hultén, K. G. et al. Analysis of invasive community-acquired methicillin-susceptible *Staphylococcus aureus* infections during a period of declining community acquired methicillin-resistant *Staphylococcus aureus* infections at a large children's hospital. *Pediatr. Infect. Dis. J.* **37**, 235–241 (2018).
50. Chen, X. et al. Synergistic effect of antibacterial agents human β-defensins, cathelicidin LL-37 and lysozyme against *Staphylococcus aureus* and *Escherichia coli*. *J. Dermatol. Sci.* **40**, 123–132 (2005).
51. Aguilar-Colomer, A. et al. Antibacterial effect of antibiotic-loaded SBA-15 on biofilm formation by *Staphylococcus aureus* and *Staphylococcus epidermidis*. *J. Antibiotics* **70**, 259–263 (2017).
52. Li, L. I. & Wang, H. Enzyme-coated mesoporous silica nanoparticles as efficient antibacterial agents in vivo. *Adv. Healthc. Mater.* **2**, 1351–1360 (2013).
53. Fernandes, M. M. et al. Nanotransformation of vancomycin overcomes the intrinsic resistance of gram-negative bacteria. *ACS Appl. Mater. Interfaces* **9**, 15022–15030 (2017).
54. Qi, G., Li, L., Yu, F. & Wang, H. Vancomycin-modified mesoporous silica nanoparticles for selective recognition and killing of pathogenic gram-positive bacteria over macrophage-like cells. *ACS Appl. Mater. Interfaces* **5**, 10874–10881 (2013).
55. Aguilar-Colomer, A. et al. Impact of the antibiotic-cargo from MSNs on gram-positive and gram-negative bacterial biofilms. *Microporous Mesoporous Mater.* **311**, 110681 (2021).
56. Gounani, Z., Asadollahi, M. A., Meyer, R. L. & Arpanaei, A. Loading of polymyxin B onto anionic mesoporous silica nanoparticles retains antibacterial activity and enhances biocompatibility. *Int. J. Pharmaceut.* **537**, 148–161 (2018).
57. Luo, G.-F. et al. Multifunctional enveloped mesoporous silica nanoparticles for subcellular co-delivery of drug and therapeutic peptide. *Sci. Rep.* **4**, 6064 (2014).
58. Pan, L. et al. Nuclear-targeted drug delivery of TAT peptide-conjugated monodisperse mesoporous silica nanoparticles. *J. Am. Chem. Soc.* **134**, 5722–5725 (2012).
59. Haddad Kashani, H., Schmelcher, M., Sabzalipoor, H., Seyed Hosseini, E. & Moniri, R. Recombinant endolysins as potential therapeutics against antibiotic-resistant *Staphylococcus aureus*: Current status of research and novel delivery strategies. *Clinical microbiology reviews* **31**, 10.1128/cmr.00071–00017 (2018).
60. Jijie, R., Barras, A., Teodorescu, F., Boukherroub, R. & Szunerits, S. Advancements on the molecular design of nanoantibiotics: Current level of development and future challenges. *Mol. Syst. Des. Eng.* **2**, 349–369 (2017).
61. Fu, P. P., Xia, Q., Hwang, H.-M., Ray, P. C. & Yu, H. Mechanisms of nanotoxicity: Generation of reactive oxygen species. *J. Food Drug Anal.* **22**, 64–75 (2014).
62. Sadeghnia, H. R., Zoljalali, N., Hanafi-Bojd, M. Y., Nikoofal-Sahlabadi, S. & Malaekeh-Nikouei, B. Effect of mesoporous silica nanoparticles on cell viability and markers of oxidative stress. *Toxicol. Mech. Methods* **25**, 433–439 (2015).
63. Liu, J. Y. & Sayes, C. M. A toxicological profile of silica nanoparticles. *Toxicol. Res.* **11**, 565–582 (2022).
64. Nelson, B. C., Johnson, M. E., Walker, M. L., Riley, K. R. & Sims, C. M. Antioxidant cerium oxide nanoparticles in biology and medicine. *Antioxidants* **5**, 15 (2016).
65. Huang, X. et al. The promotion of human malignant melanoma growth by mesoporous silica nanoparticles through decreased reactive oxygen species. *Biomaterials* **31**, 6142–6153 (2010).
66. Natan, M. & Banin, E. From nano to micro: Using nanotechnology to combat microorganisms and their multidrug resistance. *FEMS Microbiol. Rev.* **41**, 302–322 (2017).

67. Wang, Z., Liu, X., Duan, Y. & Huang, Y. Infection microenvironment-related antibacterial nanotherapeutic strategies. *Biomaterials* **280**, 121249 (2022).

Author contributions

N.A., B.N.F., and A.A. devised the project, developed the main conceptual ideas, and outlined the proof. N.A., P.SH., and B.N.F. handled most of the technical details and performed the numerical calculations for the proposed experiment. All authors conducted the experiments and analyzed the data. B.N.F. and A.A. critically revised the manuscript for important intellectual content. S.M.J. wrote the manuscript, drafting the initial text, and integrating feedback from all co-authors to produce the final version. All authors provided critical feedback and contributed to shaping the research, analysis, and manuscript.

Funding

This article did not receive financial support from any organization.

Declarations

Competing interests

The authors declare no competing interests.

Consent for publication

Not applicable.

Additional information

Correspondence and requests for materials should be addressed to B.N.F., S.M.J. or A.A.

Reprints and permissions information is available at www.nature.com/reprints.

Publisher's note Springer Nature remains neutral with regard to jurisdictional claims in published maps and institutional affiliations.